College of Basic Education Research Journal

https://berj.uomosul.edu.iq/

Effect of Inclination and Magnetic Field of a Fluid Flow in a Square Channel with a Solid Body

Maryam M. Mohammed **Alaa A. Hammodat**

Department of Mathematics, College Education of Pure Science, Mosul University, Mosul, Iraq.

Article Information

Article history:
Received: February 18,2025
Reviewer: March 14, 2025
Accepted: March 18, 2025
Available online: June, 2026

Keywords:
Angle inclination,
Thermal radiation,
convection,
Alternative direction explicit method,
Prandtle number.

Correspondence:
Maryam M. Mohammed
Email:
Maryam.23esp80@student.uomosul.edu.iq

Abstract

This study examined fluid flow and heat transfer through natural convection and thermal radiation in both horizontal and inclined scenarios within a porous channel, which included a square isolating body at its center, under influence of a magnetic field orthogonal to channel. The fluid examined is considered to be incompressible, laminar, and stable. Temperature of left wall of channel is higher than right, but bottom and top walls are heat isolated. Energy, momentum, and continuity governing equations were shown using finite difference techniques. Issue is modelled, and equations that govern it are solved using MATLAB software that utilizes alternate direction explicit method (ADEM). Finally, effects of changes in governing parameters on temperature and velocity have been considered. These effects include radiation parameter, Rayleigh number, Darcy number, Hartmann number, angle of inclination, and Prandtl parameter.

P-ISSN: 1992–7452 **E-ISSN:** 2664-2808

تأثير الميلان والمجال المغناطيسي على تدفق مائع داخل قناة مربعة تحتوي على جسم صلب

مريم مثنى محمد **علاء عبد الرحيم حمودات**

قسم الرياضيات، كلية التربية للعلوم الصرفة، جامعة الموصل، الموصل، العراق.

المستخلص

تناولت هذه الدراسة تدفق الموائع وانتقال الحرارة عبر الحمل الحراري الطبيعي والإشعاع الحراري في كل من الوضعين الأفقي والمائل داخل قناة مسامية، التي تضمنت جسمًا عازلًا مربعًا في مركزها، تحت تأثير مجال مغناطيسي متعامد مع القناة. يُعتبر المائع الذي يتم فحصه غير قابل للانضغاط، وصفحي، ومستقر. تكون درجة حرارة الجدار الأيسر للقناة مرتفعة أكثر من درجة حرارة الجدار الأيمن، أما الجدران السفلية والعلوية فهي معزولة حراريًا. تم عرض معادلات الطاقة وكمية الحركة والاستمرارية الحاكمة باستخدام طرق الفروق المحددة. يتم نمذجة المشكلة، ويتم حل المعادلات التي تحكمها باستخدام برنامج MATLAB الذي يستخدم الطريقة الصريحة ذات الاتجاه البديل (ADEM). وأخيرًا، تم النظر في تأثيرات التغير في البارامترات الحاكمة على درجة الحرارة والسرعة. تتضمن هذه التأثيرات بارامتر الإشعاع، وعدد رايلي، وعدد دارسي، وعدد هارتمان، وزاوية الميل، وبارامتر براندتل.

الكلمات المفتاحية: زاوية الميلان، الإشعاع الحراري، الحمل الحراري، طريقة الاتجاهات المتناوبة الصريحة، عدد برانتل.

1. Introduction:

The primary objective of the topic of study known as magnetohydrodynamics (MHD) is to review and analyze electrically conductive fluid movements when subjected to a field of magnets. Blood constitutes one of these fluids, composed of liquid metals such as boiling iron and mercurial and ionized particles such as those in the environment of the solar system. Examples of the MHD idea in action are the generator and drive. The numerical estimates for natural convection heat transfer in not fully open, to some degree inclined cavity with a perpendicular isothermal wall and remaining walls adiabatically, that the inclination angle and Rayleigh number of the cavity had a significant effect on temperature fields and flow patterns (Hinojosa Palafox, 2012). The unstable MHD dynamic turbulent rates in a descending channel have become the subject of several investigations. These academic studies are predicated on the idea that exploration on such flows has several implications for an eclectic choice of fields that are stimulating to science. These uses comprise liquid metal cooling of reactors, MHD power production, MHD pumps, and magnetic drug targeting. Numerous studies in this area have been beneficial (Joseph et al., 2015).

In connection with radiation from heat, Karthikeyan investigated the unstable magneto-convection flow of an artificially directed fluid through a semi-unlimited perpendicular squishy disc immersed in a porous substrate containing time-reliant vacuum (Karthikeyan, 2013). The mass and heating features of a sticky, incompressible, free convective fluid that is dynamically variable, radiant, and energetically accompanied while traversing an exceptionally chaotic porous terrain (Veeresh et al., 2015). an analytical study on an unregulated porosity straight area surrounding an irregularly permeable item with different susceptibilities (Ibrahim & Suneetha, 2016). Employing an implicit finite variation approach, the consequence of exposure to radiation, interactions between chemicals, and Soret-Dufour on an erratic motion of an MHD of an incompressible, sticky, and electrically charged gritty fluid across a continuously shifting inclination plate (Pandya et al., 2017).

The typical turbulent flow of a tiny liquid's technology in an inverted cubic containment with a substantially absorbed transparent substrate with varying oscillatory frequency on both facing edges is examined using the Boussinesq approximation and Darcy's formula (Alsabery et al., 2017). Evaluated unsteady MHD fluid flow above a vertical construction in multiple planes (Tarammim et al., 2020). The method of lines was actually employed to solve some partial differential equations that describe the fluid flow in a bridge when an electrical field (EMF) is present (Hammodat et al., 2021).

In addition, we hope to illustrate how temperature behaves inside the cross-section and the impact of physical quantities. A Cu-water tiny fluid in a differentially heated enclosure with an insulated cube of elevation ly and depth lx (ly = lx = 0.2) positioned in the center has yielded arithmetic findings for radiation heat transmission along with free convection.

Described the effects of MHD and the porous medium on the exact solutions of partial Casson liquid that travels along a channel. The flow is facilitated by the motion of the bottom sheet's fluid, yet unstable and limited by straight, although sloping, edges (Sunthrayuth et al., 2022). In a deployable opposite rectangular grid, computationally transient related mass and heat exchange by mixed convection flow (Algwauish et al., 2023). Thermal radiation affected the usual convection of fluid in a cavity that was differentially intense and had solid block inserts. They looked at both steady and unstable situations when a magnetic field was present. We find that in all cases, the influence of different factors is substantial. This study aims to show how a magnetic field and an angle of inclination affect fluid stream and heat transmission through thermal radiation and natural convection in a vertical section of an inclined channel that is heated from left to right and includes solid block inserts. The physical parameters influencing the problem are explored together with the impact of the angle's inclination (Fadel & Hammodat, 2024) (Fadel & Hammodat, 2025).

2. Mathematical Model of the Flow:

The physical configuration of the current problem was given by a diagram design of a two-dimensional inclined rectangular channel with width and height that included an equilateral isolated body with side length and centered in the channel. The outer channel's left and right walls have constant but variable temperatures, T_{hot} and T_{cold} respectively. It is considered that the upper and lower walls of the enclosure are totally segregated. A fluid is poured into the channel. $\bar{u}$ and $\bar{v}$, are the velocities described by the $\bar{x}$ and $\bar{y}$ directions, accordingly. Both the gravitational and the magnetic fields contribute to the downward tendency, which splits into two halves because of the inclination. In the Boussinesq approximation, density fluctuation in the buoyancy duration is excluded, and the fluid's thermophysical properties are considered to remain constant. Additionally, as illustrated in Figure 1, the present investigation assumes that glutinous dissipation is disregarded. The fluid flow and the transfer of heat of the enclosure's fluids in two directions by natural convection are explained by the following motion, energy, and continuity equations:

Continuity equation:

$$\frac{\partial \bar{u}}{\partial \bar{x}} + \frac{\partial \bar{v}}{\partial \bar{y}} = 0 \qquad (1).$$

Momentum equation:

$\bar{x} -$ direction

$$\bar{u}\frac{\partial \bar{u}}{\partial \bar{x}} + \bar{v}\frac{\partial \bar{u}}{\partial \bar{y}} = -\frac{1}{\rho}\frac{\partial \bar{p}}{\partial \bar{x}} + \upsilon\nabla^2\bar{u} + \frac{\sigma B_0^2}{\rho}\bar{v}\sin\theta + -g\beta(\bar{T} - \bar{T}_{Cold})\sin\theta - \frac{\upsilon}{k}\bar{u} \quad (2).$$

$\bar{y} -$ direction

$$\bar{u}\frac{\partial \bar{v}}{\partial \bar{x}} + \bar{v}\frac{\partial \bar{v}}{\partial \bar{y}} = -\frac{1}{\rho}\frac{\partial \bar{p}}{\partial \bar{y}} + \upsilon\nabla^2\bar{v} - \frac{\sigma B_0^2}{\rho}\bar{v}\cos\theta - g\beta(\bar{T} - \bar{T}_{Cold})\cos\theta \qquad (3).$$

So, the general momentum equation is as follows:

$$\left(\frac{\partial}{\partial \bar{x}}\left(\bar{u}\frac{\partial \bar{v}}{\partial \bar{x}} + \bar{v}\frac{\partial \bar{v}}{\partial \bar{y}}\right) - \frac{\partial}{\partial \bar{y}}\left(\bar{u}\frac{\partial \bar{u}}{\partial \bar{x}} + \bar{v}\frac{\partial \bar{u}}{\partial \bar{y}}\right)\right) = \upsilon\nabla^2\left(\frac{\partial \bar{v}}{\partial \bar{x}} - \frac{\partial \bar{u}}{\partial \bar{y}}\right) + \frac{\sigma B_0^2}{\rho}\left(\frac{\partial \bar{v}}{\partial \bar{x}}\cos\theta - \frac{\partial \bar{v}}{\partial \bar{y}}\sin\theta\right)$$

$$+ g\beta\left(\frac{\partial \bar{T}}{\partial \bar{x}}\cos\theta - \frac{\partial \bar{T}}{\partial \bar{y}}\sin\theta\right) + \frac{\upsilon}{k}\frac{\partial \bar{u}}{\partial \bar{y}} \qquad (4).$$

Energy equation:

$$\bar{u}\frac{\partial \bar{T}}{\partial \bar{x}} + \bar{v}\frac{\partial \bar{T}}{\partial \bar{y}} = \alpha\nabla^2\bar{T} - \frac{1}{\rho C_P}\left(\frac{\partial \overline{q_r}}{\partial \bar{x}} + \frac{\partial \overline{q_r}}{\partial \bar{y}}\right) \qquad (5),$$

Here is the heat flux resulting from radiation in the $\bar{x}$ and $\bar{y}$directions:

$\overline{q_r} = \frac{-4\sigma^*}{3k^*}\bar{T}_x^4$ and $\overline{q_r} = \frac{-4\sigma^*}{3k^*}\bar{T}_y^4$, hence equation (5):

$$\bar{u}\frac{\partial \bar{T}}{\partial \bar{x}} + \bar{v}\frac{\partial \bar{T}}{\partial \bar{y}} = \left(1 + \frac{16\sigma^*\bar{T}_{cold}^3}{3k^*\rho C_p}\right)\nabla^2\bar{T} \qquad (6).$$

$\rho, \nabla^2, \upsilon, k, \mathcal{P}, \mathcal{B}_o, \sigma, g, \beta, \bar{T}, \alpha, C_p, k^*, \sigma^*$ Density, Laplacian, kinematic viscosity, media porosity, pressure, constant magnetic field, electric conductivity, acceleration, factor of expansion from heat, temperature, thermal diffusivity, Particular heat at constant tension, average ratio of absorbance, and Boltzmann-Steinmann coefficient are the factors to be assessed.

With the corresponds boundary conditions are:

$$\left.\begin{array}{ll} on\ each\ solid\ boundaries: & \bar{u} = \bar{v} = 0 \\ on\ \bar{x} = 0, d, 0 \le \bar{y} \le d: & \bar{T} = \bar{T}_{hot}, \bar{T}_{cold} \\ on\ \bar{y} = 0, d, 0 \le \bar{x} \le d: & \dfrac{\partial \bar{T}}{\partial \bar{y}} = 0 \end{array}\right\} \qquad (7).$$

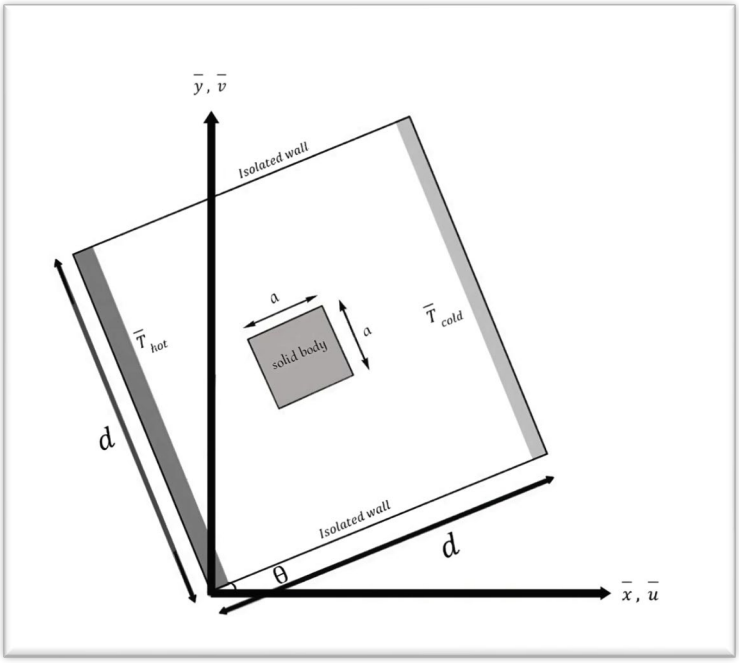

Fig.1. A Diagrammatic Description of the Container

3. Mathematical Formulation:

The equations that govern (1), (4), and (6) must be made without dimension since the approach known as finite difference will be employed to resolve them over the boundary (7) requirements. The following dimensionless quantities are now introduced for this purpose (Pandya et al., 2017).

$$\bar{u} = \frac{\alpha}{d}\bar{\bar{u}}, \bar{v} = \frac{\alpha}{d}\bar{\bar{v}}, \bar{x} = d\bar{\bar{x}}, \bar{y} = d\bar{\bar{y}}, \bar{\bar{T}} = \frac{\bar{T}-\bar{T}_{cold}}{\bar{T}_{hot}-\bar{T}_{cold}} \Big\} \qquad (8).$$

With the aid of these linkages, the subsequent derivatives

$$\frac{\partial \bar{u}}{\partial \bar{x}} = \frac{\partial \bar{u}}{\partial \bar{\bar{x}}}\frac{\partial \bar{\bar{x}}}{\partial \bar{x}} = \frac{\partial(\frac{\alpha}{d}\bar{\bar{u}})}{\partial \bar{\bar{x}}}\frac{\partial \bar{\bar{x}}}{\partial(d\bar{\bar{x}})} = \left(\frac{\alpha}{d^2}\right)\frac{\partial \bar{\bar{u}}}{\partial \bar{\bar{x}}}, \frac{\partial \bar{v}}{\partial \bar{y}} = \frac{\partial \bar{v}}{\partial \bar{\bar{y}}}\frac{\partial \bar{\bar{y}}}{\partial \bar{y}} = \frac{\partial(\frac{\alpha}{d}\bar{\bar{v}})}{\partial \bar{\bar{y}}}\frac{\partial \bar{\bar{y}}}{\partial(d\bar{\bar{y}})}\left(\frac{\alpha}{d^2}\right)\frac{\partial \bar{\bar{v}}}{\partial \bar{\bar{y}}}$$

$$\frac{\partial \bar{u}}{\partial \bar{y}} = \frac{\partial \bar{u}}{\partial \bar{\bar{y}}}\frac{\partial \bar{\bar{y}}}{\partial \bar{x}} = \frac{\partial(\frac{\alpha}{d}\bar{\bar{u}})}{\partial \bar{\bar{y}}}\frac{\partial \bar{\bar{y}}}{\partial(d\bar{\bar{y}})} = \left(\frac{\alpha}{d^2}\right)\frac{\partial \bar{\bar{u}}}{\partial \bar{\bar{y}}}, \frac{\partial \bar{v}}{\partial \bar{x}} = \frac{\partial \bar{v}}{\partial \bar{\bar{x}}}\frac{\partial \bar{\bar{x}}}{\partial \bar{x}} = \frac{\partial(\frac{\alpha}{d}\bar{\bar{v}})}{\partial \bar{\bar{x}}}\frac{\partial \bar{\bar{x}}}{\partial(d\bar{\bar{x}})}\left(\frac{\alpha}{d^2}\right)\frac{\partial \bar{\bar{v}}}{\partial \bar{\bar{x}}}$$

$$\frac{\partial}{\partial \bar{x}}\left(\frac{\partial \bar{u}}{\partial \bar{x}}\right) = \frac{\partial}{\partial \bar{\bar{x}}}\frac{\partial \bar{\bar{x}}}{\partial \bar{x}}\left(\frac{\partial \bar{u}}{\partial \bar{\bar{x}}}\frac{\partial \bar{\bar{x}}}{\partial \bar{x}}\right) = \left(\frac{\alpha}{d^3}\right)\frac{\partial}{\partial \bar{\bar{x}}}\left(\frac{\partial \bar{\bar{u}}}{\partial \bar{\bar{x}}}\right), \frac{\partial}{\partial \bar{y}}\left(\frac{\partial \bar{u}}{\partial \bar{y}}\right) = \frac{\partial}{\partial \bar{\bar{y}}}\frac{\partial \bar{\bar{y}}}{\partial \bar{y}}\left(\frac{\partial \bar{u}}{\partial \bar{\bar{y}}}\frac{\partial \bar{\bar{y}}}{\partial \bar{y}}\right) = \left(\frac{\alpha}{d^3}\right)\frac{\partial}{\partial \bar{\bar{y}}}\left(\frac{\partial \bar{\bar{u}}}{\partial \bar{\bar{y}}}\right)$$

$$\frac{\partial}{\partial \bar{x}}\left(\frac{\partial \bar{v}}{\partial \bar{x}}\right) = \frac{\partial}{\partial \bar{\bar{x}}}\frac{\partial \bar{\bar{x}}}{\partial \bar{x}}\left(\frac{\partial \bar{v}}{\partial \bar{\bar{x}}}\frac{\partial \bar{\bar{x}}}{\partial \bar{x}}\right) = \left(\frac{\alpha}{d^3}\right)\frac{\partial}{\partial \bar{\bar{x}}}\left(\frac{\partial \bar{\bar{v}}}{\partial \bar{\bar{x}}}\right), \frac{\partial}{\partial \bar{y}}\left(\frac{\partial \bar{v}}{\partial \bar{y}}\right) = \frac{\partial}{\partial \bar{\bar{y}}}\frac{\partial \bar{\bar{y}}}{\partial \bar{y}}\left(\frac{\partial \bar{v}}{\partial \bar{\bar{y}}}\frac{\partial \bar{\bar{y}}}{\partial \bar{y}}\right)\left(\frac{\alpha}{d^3}\right)\frac{\partial}{\partial \bar{\bar{y}}}\left(\frac{\partial \bar{\bar{v}}}{\partial \bar{\bar{y}}}\right)$$

$$\frac{\partial}{\partial \bar{x}}\left(\frac{\partial \bar{v}}{\partial \bar{y}}\right) = \frac{\partial}{\partial \bar{\bar{x}}}\frac{\partial \bar{\bar{x}}}{\partial \bar{x}}\left(\frac{\partial \bar{v}}{\partial \bar{\bar{y}}}\frac{\partial \bar{\bar{y}}}{\partial \bar{y}}\right) = \left(\frac{\alpha}{d^3}\right)\frac{\partial}{\partial \bar{\bar{x}}}\left(\frac{\partial \bar{\bar{v}}}{\partial \bar{\bar{y}}}\right), \frac{\partial}{\partial \bar{y}}\left(\frac{\partial \bar{u}}{\partial \bar{x}}\right) = \frac{\partial}{\partial \bar{\bar{y}}}\frac{\partial \bar{\bar{y}}}{\partial \bar{y}}\left(\frac{\partial \bar{u}}{\partial \bar{\bar{x}}}\frac{\partial \bar{\bar{x}}}{\partial \bar{x}}\right) = \left(\frac{\alpha}{d^3}\right)\frac{\partial}{\partial \bar{\bar{y}}}\left(\frac{\partial \bar{\bar{u}}}{\partial \bar{\bar{x}}}\right)$$

$$\frac{\partial \bar{T}}{\partial \bar{x}} = \frac{\partial \bar{T}}{\partial \bar{\bar{x}}}\frac{\partial \bar{\bar{x}}}{\partial \bar{x}} = \frac{\partial(\Delta\bar{T}\bar{\bar{T}}+\bar{T}_{cold})}{\partial \bar{\bar{x}}}\frac{\partial \bar{\bar{x}}}{\partial(d\bar{\bar{x}})} = \left(\frac{\Delta\bar{T}}{d}\right)\frac{\partial \bar{\bar{T}}}{\partial \bar{\bar{x}}},$$
$$\frac{\partial \bar{T}}{\partial \bar{y}} = \frac{\partial \bar{T}}{\partial \bar{\bar{y}}}\frac{\partial \bar{\bar{y}}}{\partial \bar{y}} = \frac{\partial(\Delta\bar{T}\bar{\bar{T}}+\bar{T}_{cold})}{\partial \bar{\bar{y}}}\frac{\partial \bar{\bar{y}}}{\partial(d\bar{\bar{y}})} = \left(\frac{\Delta\bar{T}}{d}\right)\frac{\partial \bar{\bar{T}}}{\partial \bar{\bar{y}}}$$

After simplifying, the following pair of nonlinear paired partial differential equations with regard to the dimensions of the variables are obtained by substituting the values of the aforementioned derivatives into equations (1), (4), and (6):

$$\frac{\partial \bar{\bar{u}}}{\partial \bar{\bar{x}}} + \frac{\partial \bar{\bar{v}}}{\partial \bar{\bar{y}}} = 0 \qquad (9).$$

$$\left(\frac{\partial}{\partial \bar{\bar{x}}}\left(\bar{\bar{u}}\frac{\partial \bar{\bar{v}}}{\partial \bar{\bar{x}}} + \bar{\bar{v}}\frac{\partial \bar{\bar{v}}}{\partial \bar{\bar{y}}}\right) - \frac{\partial}{\partial \bar{\bar{y}}}\left(\bar{\bar{u}}\frac{\partial \bar{\bar{u}}}{\partial \bar{\bar{x}}} + \bar{\bar{v}}\frac{\partial \bar{\bar{u}}}{\partial \bar{\bar{y}}}\right)\right) = \cdots$$
$$\ldots = Pr\nabla^2\left(\frac{\partial \bar{\bar{v}}}{\partial \bar{\bar{x}}} - \frac{\partial \bar{\bar{u}}}{\partial \bar{\bar{y}}}\right) + M^2 Pr\left(\frac{\partial \bar{\bar{v}}}{\partial \bar{\bar{x}}}\cos\theta - \frac{\partial \bar{\bar{v}}}{\partial \bar{\bar{y}}}\sin\theta\right) - \cdots$$
$$-Ra\left(\frac{\partial \bar{\bar{T}}}{\partial \bar{\bar{x}}}\cos\theta - \frac{\partial \bar{\bar{T}}}{\partial \bar{\bar{y}}}\sin\theta\right) + \frac{Pr}{Da}\frac{\partial \bar{\bar{u}}}{\partial \bar{\bar{y}}} \qquad (10).$$
$$\bar{\bar{u}}\frac{\partial \bar{\bar{T}}}{\partial \bar{\bar{x}}} + \bar{\bar{v}}\frac{\partial \bar{\bar{T}}}{\partial \bar{\bar{y}}} = \left(1 + \frac{16\sigma^*\bar{T}_{cold}^3}{3k^*\rho C_p}\right)\nabla^2\bar{\bar{T}} \qquad (11).$$

Where

$$Pr = \frac{\upsilon}{\alpha}, M = \mathcal{B}_o d\left(\frac{\sigma}{\mu}\right)^{\frac{1}{2}}, Da = \frac{k}{d^2}, Ra = \frac{g\beta\Delta\bar{T}d^3}{\alpha^2}, Rd = 1 + \frac{16\sigma^*\bar{T}_{cold}^3}{3k^*\rho C_p}\Bigg\} \quad (12).$$

Are Prandtl number, Hartmann number, Darcy number, Rayleigh number, and Thermal radiation respectively. Also, the boundary conditions of equations as follows:

$$\left.\begin{array}{ll} \text{on the left wall:} & \bar{\bar{u}} = \bar{\bar{v}} = 0, \bar{\bar{T}} = 1 \\ \text{on the right wall:} & \bar{\bar{u}} = \bar{\bar{v}} = 0, \bar{\bar{T}} = 0 \\ \text{on the insulated:} & \bar{\bar{u}} = \bar{\bar{v}} = 0, \frac{\partial \bar{\bar{T}}}{\partial \bar{\bar{y}}} = 0 \end{array}\right\} \qquad (13).$$

The stream and vorticity functions are considered to be (Rajput, 2013):

$$\bar{\bar{u}} = \frac{\partial \bar{\bar{\psi}}}{\partial \bar{\bar{y}}}, \quad \bar{\bar{v}} = -\frac{\partial \bar{\bar{\psi}}}{\partial \bar{\bar{x}}}, \ \bar{\bar{\Omega}} = \frac{\partial \bar{\bar{v}}}{\partial \bar{\bar{x}}} - \frac{\partial \bar{\bar{u}}}{\partial \bar{\bar{y}}}\Bigg\} \qquad (14).$$

Equations (9–11) and (13), when applied to the dimensionless parameters, establish the following governing equations and conditions of the boundary (12)

$$\frac{\partial^2\bar{\bar{\psi}}}{\partial\bar{\bar{x}}^2}+\frac{\partial^2\bar{\bar{\psi}}}{\partial\bar{\bar{y}}^2}=-\bar{\bar{\Omega}} \qquad (15).$$

$$\nabla^2\bar{\bar{\Omega}}=\frac{1}{Pr}\left(\frac{\partial\bar{\bar{\psi}}}{\partial\bar{\bar{y}}}\frac{\partial\bar{\bar{\Omega}}}{\partial\bar{\bar{x}}}-\frac{\partial\bar{\bar{\psi}}}{\partial\bar{\bar{x}}}\frac{\partial\bar{\bar{\Omega}}}{\partial\bar{\bar{y}}}\right)-M^2\frac{\partial^2\bar{\bar{\psi}}}{\partial\bar{\bar{x}}^2}\cos\theta+M^2\frac{\partial^2\bar{\bar{\psi}}}{\partial\bar{\bar{x}}\partial\bar{\bar{y}}}\sin\theta+\frac{Ra}{Pr}\frac{\partial\bar{\bar{T}}}{\partial\bar{\bar{x}}}\cos\theta-$$
$$\frac{Ra}{Pr}\frac{\partial\bar{\bar{T}}}{\partial\bar{\bar{y}}}\sin\theta+Da^{-1}\frac{\partial^2\bar{\bar{\psi}}}{\partial\bar{\bar{y}}^2} \qquad (16).$$

$$\nabla^2\bar{\bar{T}}=\frac{1}{Rd}\left(\frac{\partial\bar{\bar{\psi}}}{\partial\bar{\bar{y}}}\frac{\partial\bar{\bar{T}}}{\partial\bar{\bar{x}}}-\frac{\partial\bar{\bar{\psi}}}{\partial\bar{\bar{x}}}\frac{\partial\bar{\bar{T}}}{\partial\bar{\bar{y}}}\right) \qquad (17).$$

Under the conditions of constraint:

$$\left.\begin{array}{llll} & & \bar{\bar{\psi}}=0 & \\ \bar{\bar{x}}=0\ , & 0\le\bar{\bar{y}}\le 1\ , & \bar{\bar{T}}=1\ , & \bar{\bar{\Omega}}=-\frac{\partial^2\bar{\bar{\psi}}}{\partial\bar{\bar{x}}^2} \\ \bar{\bar{x}}=1\ , & 0\le\bar{\bar{y}}\le 1\ , & \bar{\bar{T}}=0\ , & \bar{\bar{\Omega}}=-\frac{\partial^2\bar{\bar{\psi}}}{\partial\bar{\bar{x}}^2} \\ \bar{\bar{y}}=0\text{،}1\ , & 0\le\bar{\bar{x}}\le 1\ , & \frac{\partial\bar{\bar{T}}}{\partial\bar{\bar{y}}}=0\ , & \bar{\bar{\Omega}}=-\frac{\partial^2\bar{\bar{\psi}}}{\partial\bar{\bar{x}}^2} \end{array}\right\} \qquad (18).$$

4. Numerical Calculations:

An EFDM and the associated boundary conditions have been used to computationally resolve a collection of irregulars, dimensionless, partial differential governing equations. A grid or net of lines identical to the $\bar{\bar{x}}$ – and $\bar{\bar{y}}$-axes divides the flow part, with the $\bar{\bar{x}}$- axis s pointing upward and the $\bar{\bar{y}}$-axes normal to the plate. We measure the height of the plate $\bar{\bar{x}}_{max}$(=100), denoting that $\bar{\bar{x}}$ varies from zero to hundred. Assuming that$\bar{\bar{y}}_{max}$(=25) as taken to $\bar{\bar{y}}\longrightarrow\infty$, this indicates that $\bar{\bar{y}}$ fluctuates within 0 and 25. Consider m = 250 and n = 250 grid spacing in the $\bar{\bar{x}}$ and $\bar{\bar{y}}$ directions, respectively. subsequently, for each smallest period of time, $\Delta\bar{\bar{x}}=0.4(0\le\bar{\bar{x}}\le 100)$ and $\Delta\bar{\bar{y}}=0.4(0\le\bar{\bar{y}}\le 25)$. When we apply an ADEM with boundary constraints (17) to the partial formulas (14)– (16), we receive (Iyengar & Jain, 2009).

$$\frac{\bar{\bar{\psi}}_{i+1,j}-2\bar{\bar{\psi}}_{i,j}+\bar{\bar{\psi}}_{i-1,j}}{(\Delta\bar{\bar{x}})^2}+\frac{\bar{\bar{\psi}}_{i,j+1}-2\bar{\bar{\psi}}_{i,j}+\bar{\bar{\psi}}_{i,j-1}}{(\Delta\bar{\bar{y}})^2}=-(\Omega)_{i,j} \qquad (19).$$

$$\frac{\bar{\bar{\Omega}}_{i+1,j}-2\bar{\bar{\Omega}}_{i,j}+\bar{\bar{\Omega}}_{i-1,j}}{(\Delta\bar{\bar{x}})^2}+\frac{\bar{\bar{\Omega}}_{i,j+1}-2\bar{\bar{\Omega}}_{i,j}+\bar{\bar{\Omega}}_{i,j-1}}{(\Delta\bar{\bar{y}})^2}=\cdots$$
$$\cdots=\frac{1}{Pr}\left(\frac{\bar{\bar{\psi}}_{i,j+1}-\bar{\bar{\psi}}_{i,j}}{\Delta\bar{\bar{y}}}\frac{\bar{\bar{\Omega}}_{i,j}-\bar{\bar{\Omega}}_{i-1,j}}{\Delta\bar{\bar{x}}}-\frac{\bar{\bar{\psi}}_{i,j}-\bar{\bar{\psi}}_{i-1,j}}{\Delta\bar{\bar{x}}}\frac{\bar{\bar{\Omega}}_{i,j+1}-\bar{\bar{\Omega}}_{i,j}}{\Delta\bar{\bar{y}}}\right)-\cdots$$

$$\dots - M^2\left(\frac{\bar{\bar{\psi}}_{i+1,j}-2\bar{\bar{\psi}}_{i,j}+\bar{\bar{\psi}}_{i-1,j}}{(\Delta\bar{\bar{x}})^2}\right)\cos\theta + M^2\frac{\bar{\bar{\psi}}_{i,j}-\bar{\bar{\psi}}_{i-1,j}}{\Delta\bar{\bar{x}}}\frac{\bar{\bar{\psi}}_{i,j+1}-\bar{\bar{\psi}}_{i,j}}{\Delta\bar{\bar{y}}}\sin\theta + \cdots$$
$$\dots + \frac{Ra}{Pr}\left(\frac{\bar{\bar{T}}_{i,j}-\bar{\bar{T}}_{i-1,j}}{\Delta\bar{\bar{x}}}\right)\cos\theta - \frac{Ra}{Pr}\frac{\bar{\bar{T}}_{i,j+1}-\bar{\bar{T}}_{i,j}}{\Delta\bar{\bar{y}}}\sin\theta + \cdots$$
$$\dots + Da^{-1}\left(\frac{\bar{\bar{\psi}}_{i,j+1}-2\bar{\bar{\psi}}_{i,j}+\bar{\bar{\psi}}_{i,j-1}}{(\Delta\bar{\bar{y}})^2}\right) \qquad (20).$$

$$\frac{\bar{\bar{T}}_{i+1,j}-2\bar{\bar{T}}_{i,j}+\bar{\bar{T}}_{i-1,j}}{(\Delta\bar{\bar{x}})^2} + \frac{\bar{\bar{T}}_{i,j+1}-2\bar{\bar{T}}_{i,j}+\bar{\bar{T}}_{i,j-1}}{(\Delta\bar{\bar{y}})^2} =$$
$$\frac{1}{Rd}\left(\frac{\bar{\bar{\psi}}_{i,j+1}-\bar{\bar{\psi}}_{i,j}}{\Delta\bar{\bar{y}}}\frac{\bar{\bar{T}}_{i,j}-\bar{\bar{T}}_{i-1,j}}{\Delta\bar{\bar{x}}} - \frac{\bar{\bar{\psi}}_{i,j}-\bar{\bar{\psi}}_{i-1,j}}{\Delta\bar{\bar{x}}}\frac{\bar{\bar{T}}_{i,j+1}-\bar{\bar{T}}_{i,j}}{\Delta\bar{\bar{y}}}\right) \qquad (21).$$

5. Results and Discussions:

The radiative effects on incompressible fluid flow and MHD natural convection inside a square channel centered on a solid body are precisely investigated in this paper. Thermal safety is maintained by the top and bottom dividers of the hollow. The problem is represented, and the governing equations are solved via a MATLAB technique that uses an ADEM. The calculated result, temperature, and velocity forms are shown below, along with the scientific explanation.

5.1 The Darcy Number Impact Da:

As the Darcy number increases, the velocity gradually decreases inside the channel when the slope angle $\theta = 0$. Similarly, when the inclination angle grows, the speed drops for a Darcy value of $Da = 0.01$, but the temperature inside the channel rises as the inclination angle and Darcy number increase, as shown in Figures 2,3,4,5.

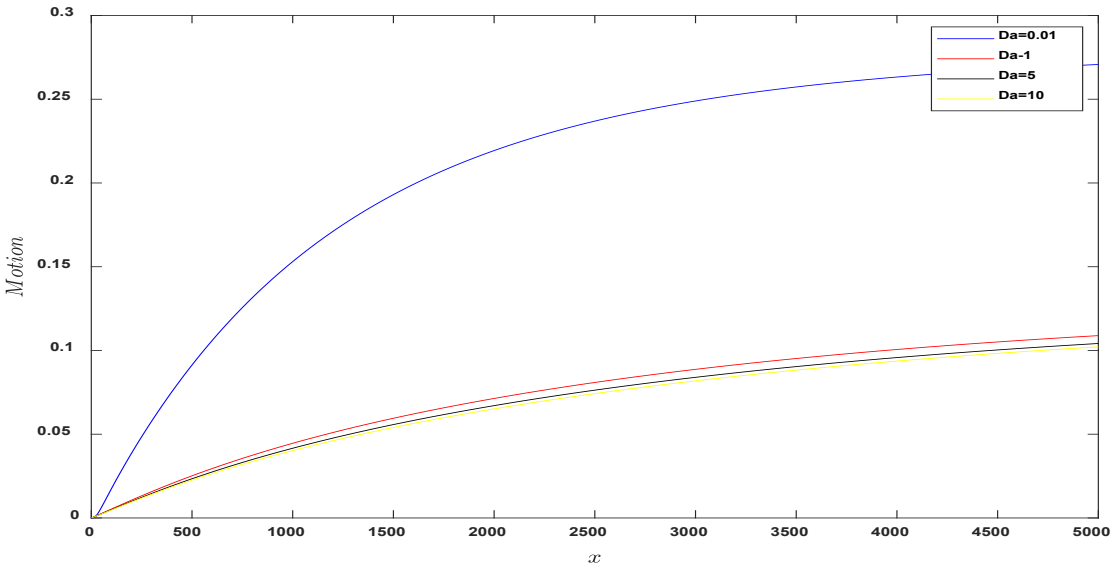

Fig.2. Velocity Shape for several values of Darcy parameter Da and $\theta = 0$

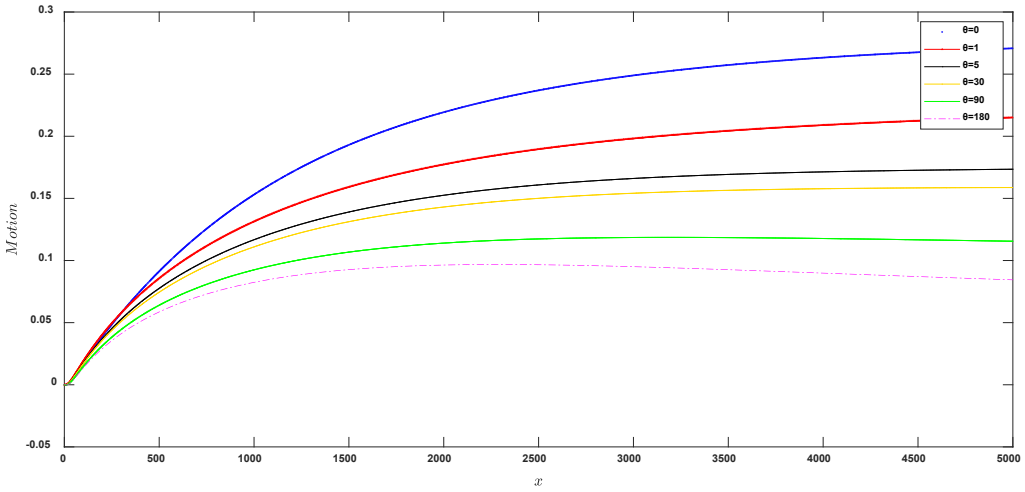

Fig.3. Velocity outline due Darcy parameter $Da = 0.01$ and $\theta = 0,1,5,30,90,180$

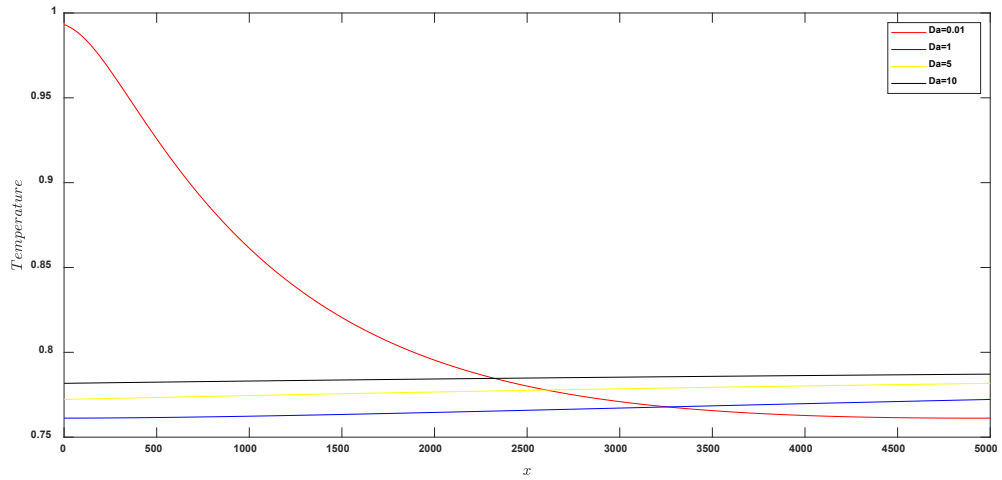

Fig.4. Temperature Profile for many values of Darcy parameter Da besides $\theta = 0$

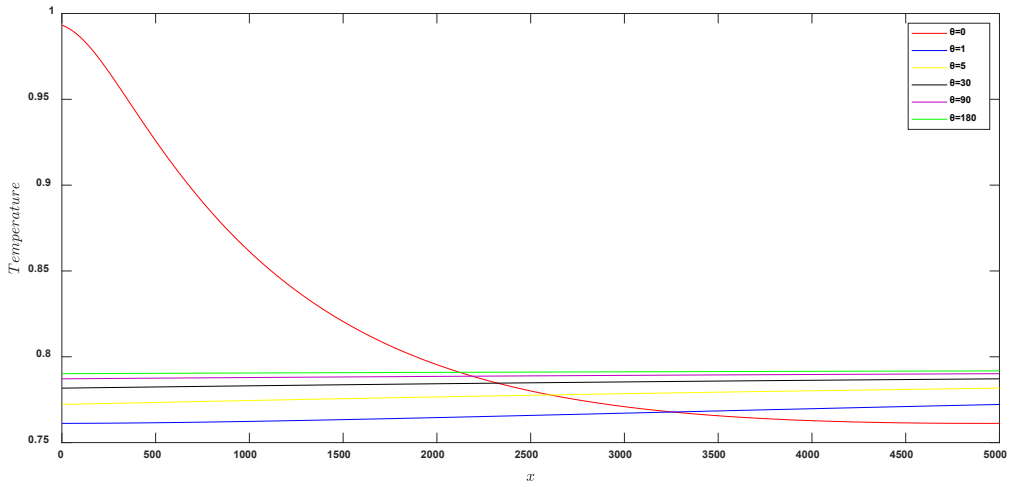

Fig.5. Temperature profile due Darcy parameter $Da = 0.01$and $\theta = 0,1,5,30,90,180$

5.2 Effect of Rayleigh Parameter Ra:

At a Rayleigh value $Ra = 1$, the temperature inside the channel rises as the Rayleigh number Ra and the inclination angle θ, respectively, increase. At an inclination angle $\theta = 5$, the velocity increases directly as the Rayleigh number inside the channel increases, while the fluid velocity gradually decreases as the channel inclination angle increases. as illustrated in Figures 6, 7, 8, and 9.

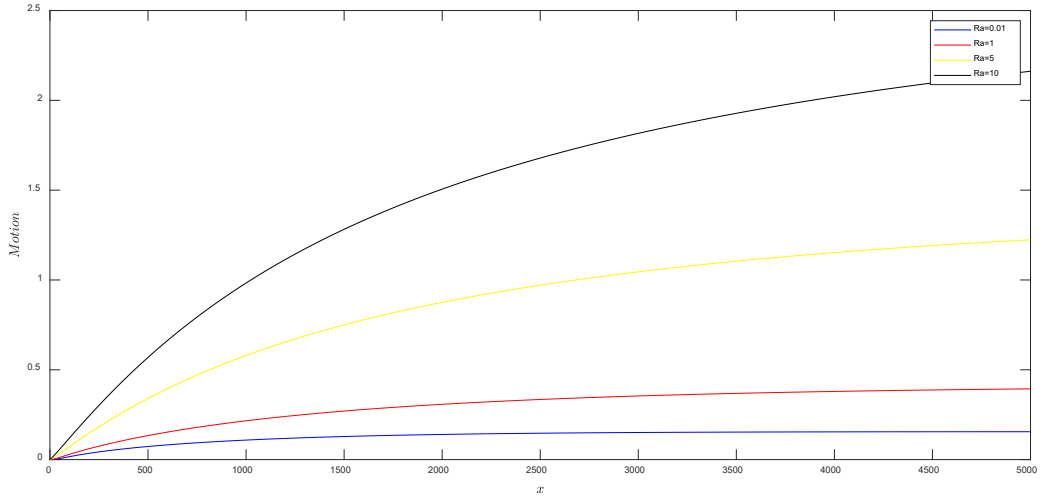

Fig.6. Velocity Curve with $\theta = 5$ and different Rayleigh parameter Ra quantities

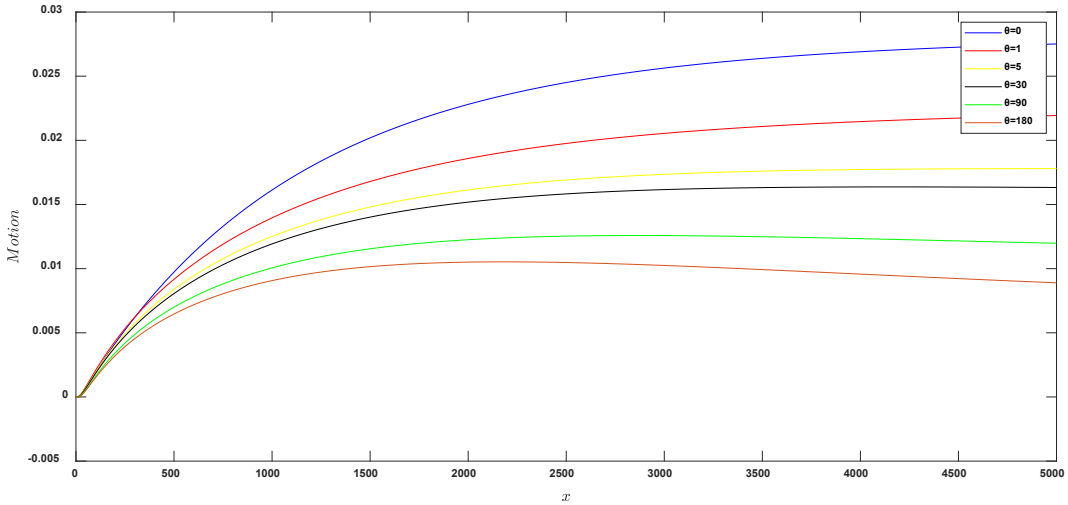

Fig.7. Rayleigh parameter $Ra = 5$ and $\theta = 0,1,5,30,90,180$ cause the velocity distribution.

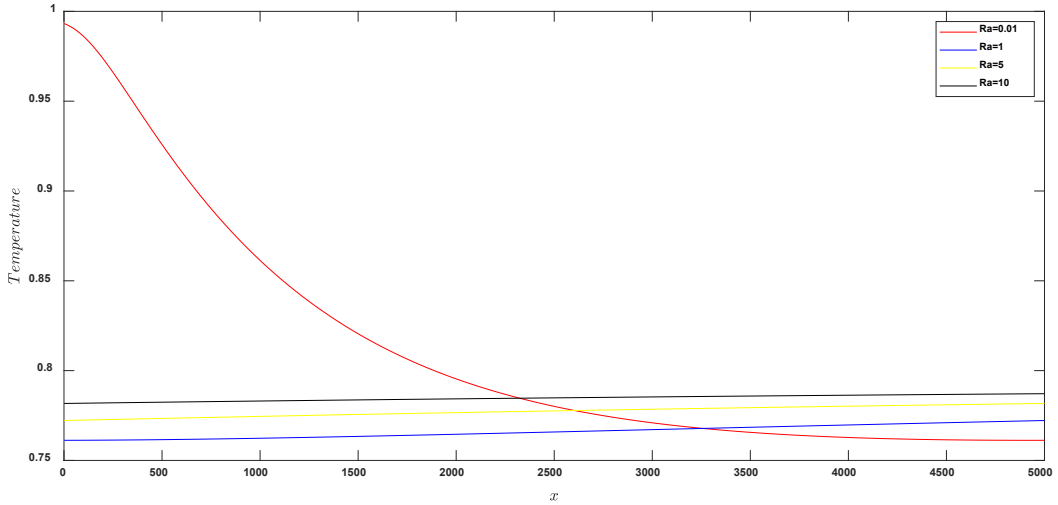

Fig.8. Temperature for different values of $\theta = 5$ and Rayleigh parameter Ra

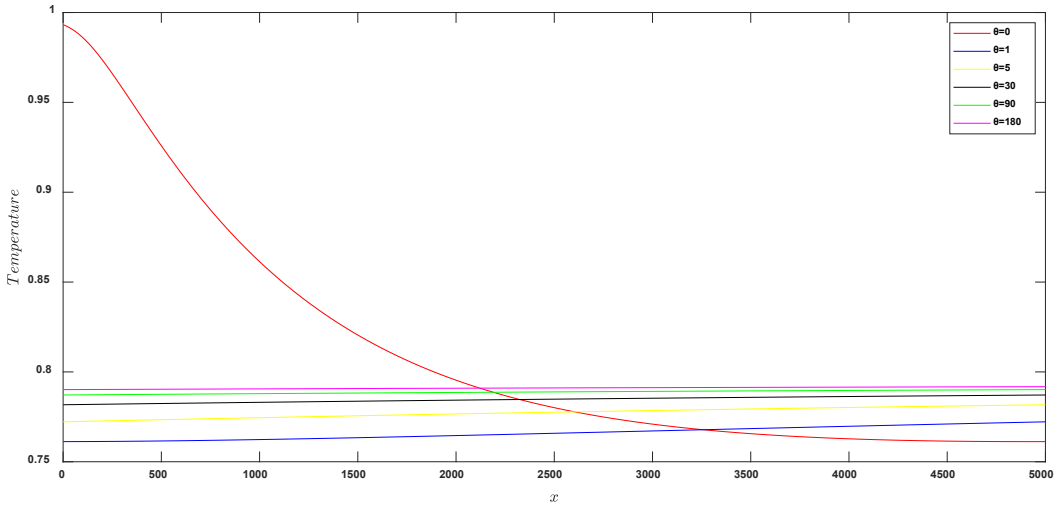

Fig.9. Temperature shape caused due to the Rayleigh parameters Ra=5 and θ=0, 1, 5, 30, 90,180

5.3 Effect of Prandtl parameter Pr:

The velocity decrease directly with the growth in the Prandtl number inside the channel when the Prandtl number rises at an inclination angle $\theta = 0$, but the fluid velocity progressively falls as the channel inclination angle rises. As the Prandtl number Pr rises at a Prandtl value $Pr = 0.01$, the temperature inside the channel rises as well, but the inclination angle little affects the air temperature. based on Figures 10, 11, 12, 13.

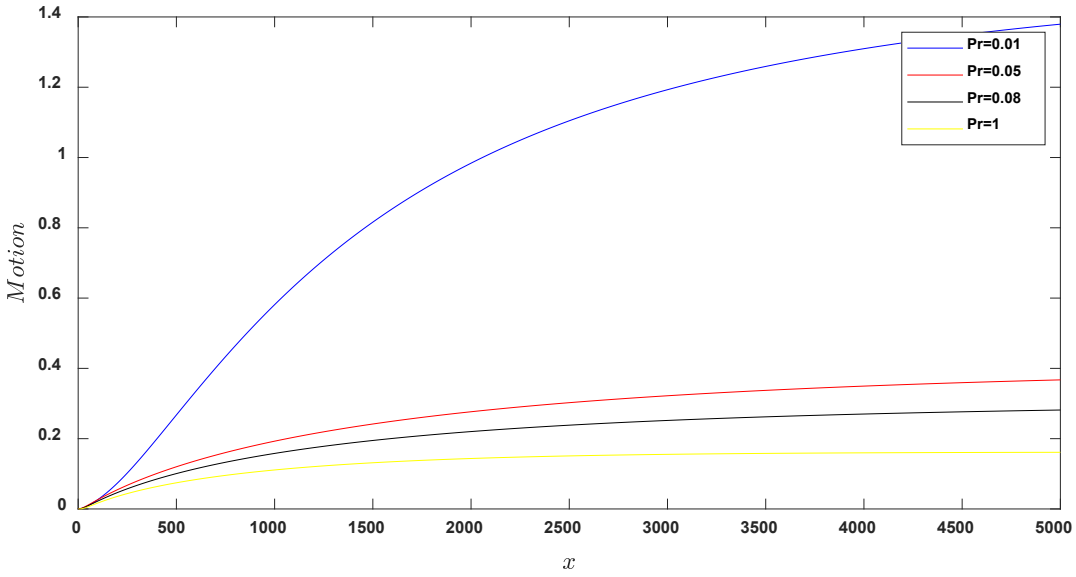

Fig.10. Profile of velocity for different Prandtl parameter values Pr = 0.01, 0.05, 0.08, 1

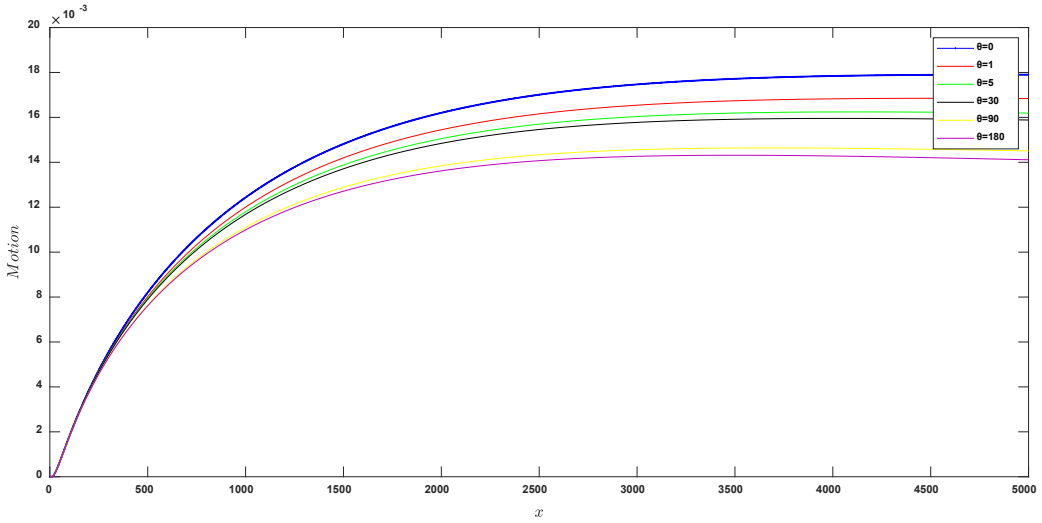

Fig.11. Velocity profile due to Prandtl number $Pr = 0.05$ and $\theta = 0,1,5,30,90,180$

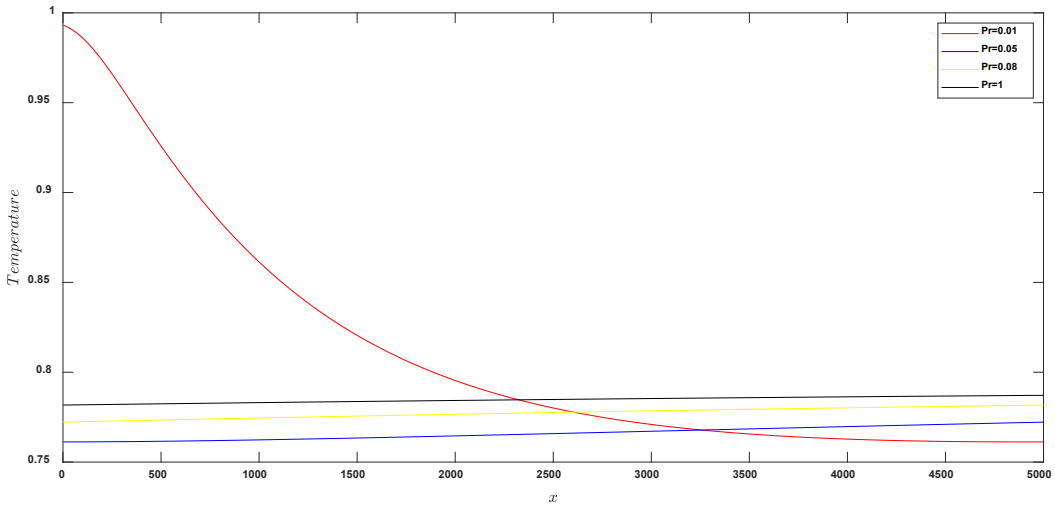

Fig.12. Temperature contour plots for numerous values of Prandtl parameter ***Pr***

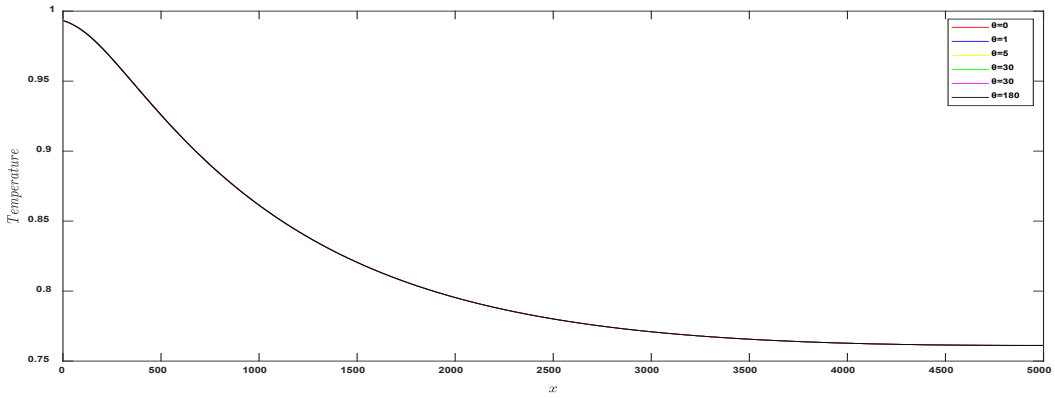

Fig.13. Temperature outline due to Prandtl number $Pr = 0.05$ and $\theta = 0,1,5,30,90,180$

5.4 Magnetic Field's Impact M:

The fluid flow grows when considering a curved channel and a low Hartmann number. Figures 14, 15, 16, and 17 illustrate that the inclination angle has a minor effect on the internal temperatures of the channel, despite the fact that the flow rate falls with increasing slope degree and Hartmann number $M = 0.01$, while the internal temperatures of the channel progressively increase with expanding Hartmann number.

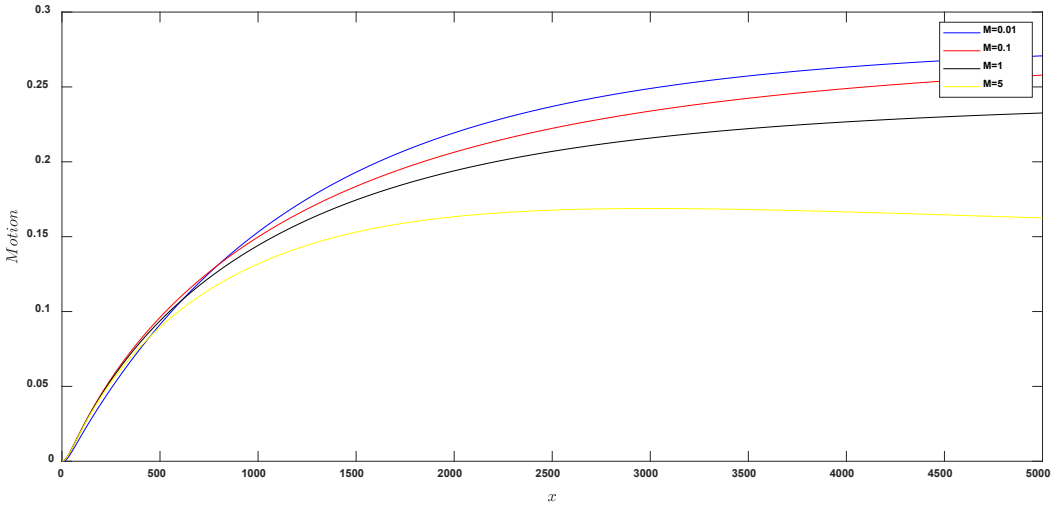

Fig.14. Velocity Profile for various values of Magnetic number M and $\theta = 0$

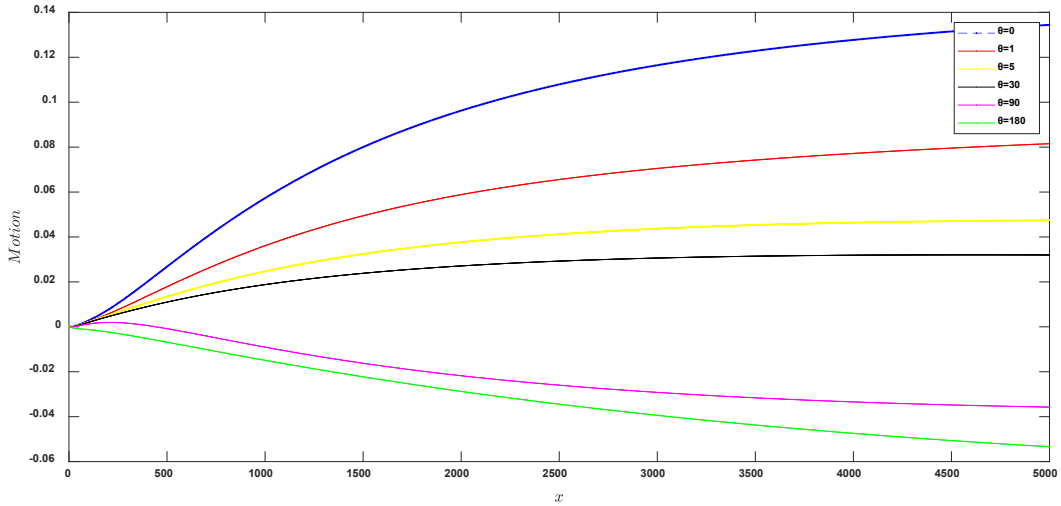

Fig.15. Velocity profile due to Magnetic number $M = 0.01$ and $\theta = 0,1,5,30,90,180$

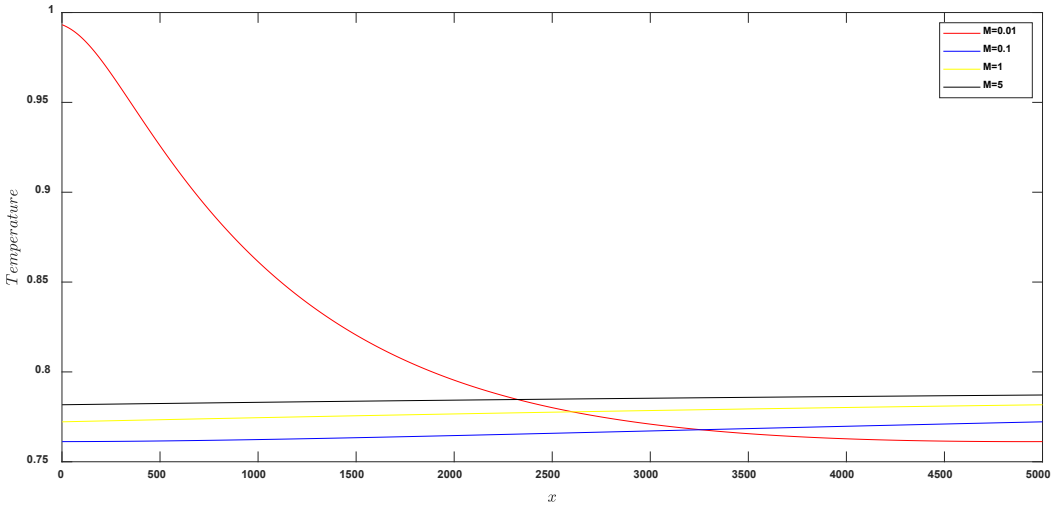

Fig.16. Profile of temperature for different magnetic number M amounts and $\theta = 0$

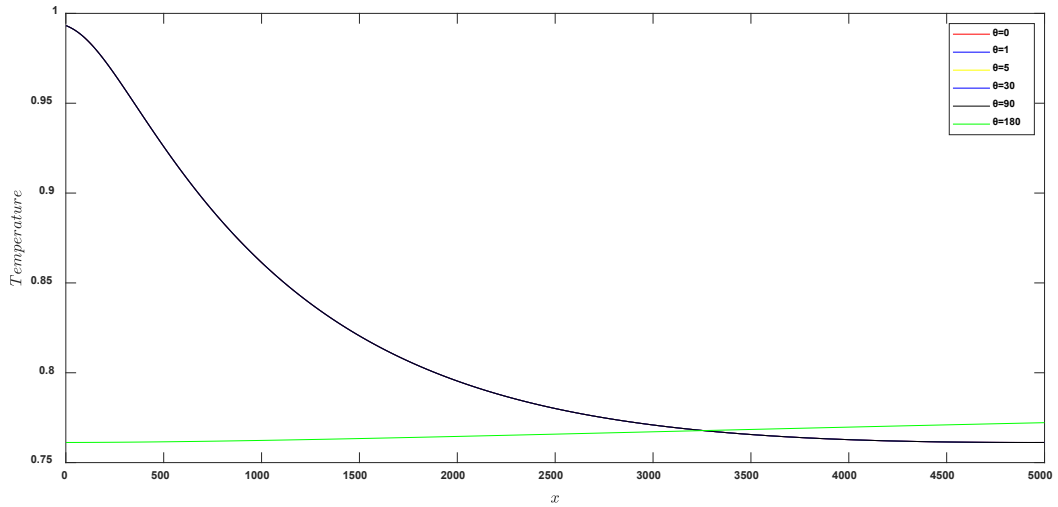

Fig.17. Magnetic number $M = 0.01$ and $\theta = 0,1,5,30,90,180$ explain the temperature gradient.

5.5 Effect of Radiation Parameter Rd:

Figures 18, 19, 20, and 21 demonstrate that when the channel inclination angle expands, the fluid rate drops when the radiated value $Rd = 30$. At an angle of inclination of $\theta = 30$, the temperature and fluid velocity likewise decrease as the radiation parameter rises; however, the channel inclination barely affects heats at $Rd = 30$.

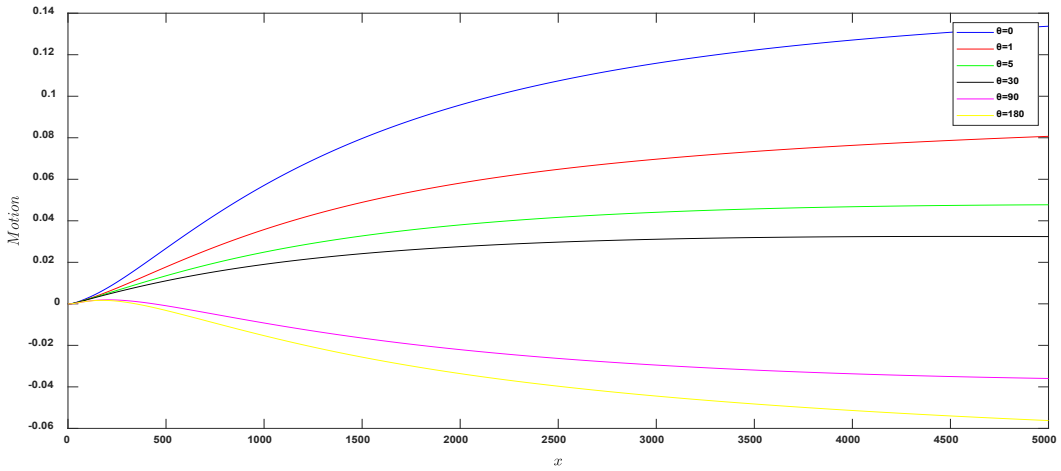

Fig.18. Speed Profile for different radiation parameter values $Rd = 30$ and $\theta = 0,1,5,30,90,180$

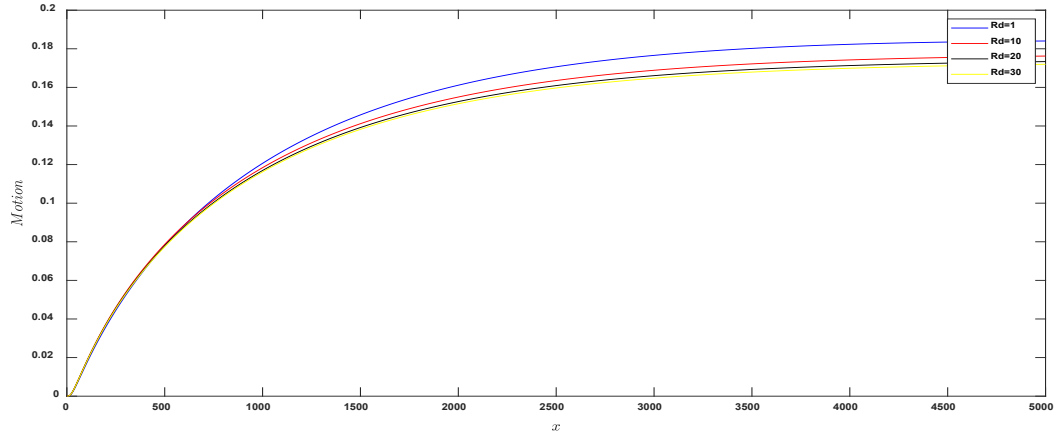

Fig.19. Velocity Profile for various values of Radiation parameter Rd and $\theta = 30$

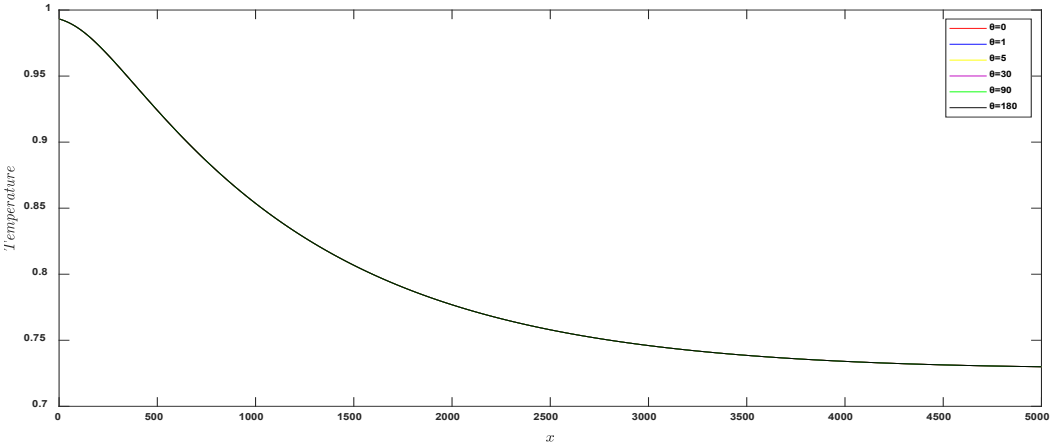

Fig.20. Temperature for various values of Radiation parameter $Rd = 30$ and $\theta = 0,1,5,30,90,180$

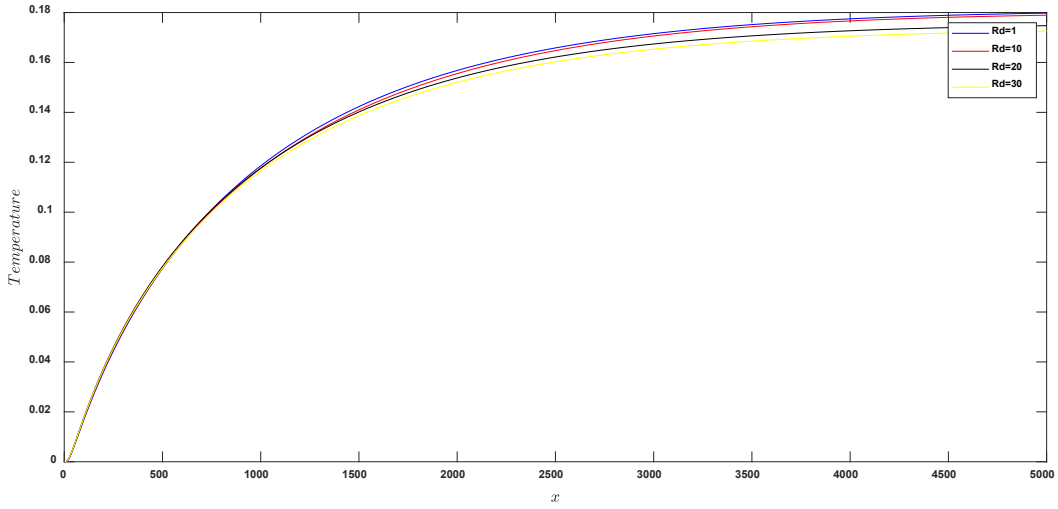

Fig.21. Temperature curve for different radiation parameters Rd and $\theta = 30$ values

6. Conclusions:

This study quantitatively examines the natural convection in a sloped permeable channel using solid block inserts when subjected to a magnetic field using a finite difference method. Research is done on the effects of various parameters and the angle of inclination of the channel. Among the primary findings of the inquiry are:

1. The velocity falls as the temperature inside the channel rises with rising Darcy number Da, Hartmann number M, and Radiation parameter Rd.
2. When the angle of inclination increases and the temperature rises, the velocity falls (Darcy number $Da = 0.01$).
3. The velocity drops as the inclination angle increases with Hartmann number $M = 0.01$, with temperature having a negligible impact.
4. The velocity drops as the inclination angle growths with the radiation parameter $Rd = 30$, and the influence of temperature is negligible.
5. Inside the channel, the temperature and velocity increase as the Rayleigh number (Ra) and Prandtl number (Pr) rise.
6. For the angle of inclination, the velocity decreases as the temperature rises for the Rayleigh number $Ra = 5$.
7. As the angle of inclination increases, the temperature is very slightly raised while the velocity drops with Prandtl number $Pr = 0.01$.

Acknowledgements:

In order to improve the quality of the project, the authors would like to thank the University of Mosul's College of Education for Pure Science.

References

Hinojosa Palafox, J. F. (2012). Numerical study of the natural convection in a two-dimensional partially open tilted cavity. *Latin American applied research*, *42*(3), 267-274.

Joseph, K. M., Peter, A., Asie, P. E., & Usman, S. (2015). The unsteady MHD free convective two immiscible fluid flows in a horizontal channel with heat and mass transfer. *International Journal of Mathematics and Computer Research*, *3*(5), 954-972.

Karthikeyan, S. (2013). Thermal radiation effects on MHD convective flow over a plate in a porous medium by perturbation technique. *Applied Mathematics and Computational Intelligence (AMCI)*, *2*(1), 75-83.

Veeresh, C., Varma, S. V. K., & Praveena, D. (2015). Heat and mass transfer in MHD free convection chemically reactive and radiative flow in a moving inclined porous plate with temperature dependent heat source and joule heating. *International Journal of Management, Information Technology and Engineering*, *3*(11), 63-74.

Ibrahim, S. M., & Suneetha, K. (2016). Effects of thermal diffusion and chemical reaction on MHD transient free convection flow past a porous vertical plate with radiation, temperature gradient dependent heat source in slip flow regime.

Pandya, N., Yadav, R. K., & Shukla, A. (2017). Combined effects of Soret–Dufour, radiation and chemical reaction on unsteady MHD flow of dusty fluid over inclined porous plate embedded in porous medium. *Int J Adv Appl Math Mech*, *5*, 49-58.

Alsabery, A. I., Chamkha, A. J., Saleh, H., & Hashim, I. (2017). Natural convection flow of a nanofluid in an inclined square enclosure partially filled with a porous medium. *Scientific reports*, *7*(1), 2357.

Tarammim, A., Ullah, M. S., & Uddin, M. J. (2020). A study of two dimensional unsteady MHD free convection flow over a vertical plate. *Open Journal of Fluid Dynamics*, *10*(04), 342.

Hammodat, A., Algwauish, G., & Al-Obaidi, I. (2021). The effects of electrical conductivity on fluid flow between two parallel plates in a porous medioum. *Iraqi Journal of Science*, 4953-4963.

Sunthrayuth, P., Alderremy, A. A., Ghani, F., Tchalla, A. M., Aly, S., & Elmasry, Y. (2022). Unsteady MHD Flow for Fractional Casson nnel Fluid in a Porous Medium: An Application of the Caputo-Fabrizio Time-Fractional Derivative. *Journal of Function Spaces*, *2022*(1), 2765924.

Algwauish, G. M., Hammodat, A. A., & Saleem, H. D. (2023). A Numerical simulation of convection and conduction heat transfer for a fluid in a porous medium. *European Journal of Pure and Applied Mathematics*, *16*(2), 833-846.

Fadel, R. N., & Hammodat, A. A. (2024, November). Numerical investigation of thermal radiation and natural convection of a fluid in a square cavity with a solid body. In *AIP Conference Proceedings* (Vol. 3229, No. 1, p. 080025). AIP Publishing LLC.

Fadel, R. N., & Hammodat, A. A. (2025, January). Study of Two-Dimensional Unsteady Natural Convection of a Fluid in a Square Cavity with a Solid Body in the Presences of Thermal Radiation. In *International Conference on Mathematical Modeling and Computational Science* (pp. 324-334). Cham: Springer Nature Switzerland.

Rajput, E. R. (2013). *A Textbook of Fluid Mechanics and Hydraulic Machines in SI Units*. S. Chand & Company Ltd.

Iyengar, S. R., & Jain, R. K. (2009). *Numerical methods*. New Age International.